Manipulation of Colloids by a Nonequilibrium Depletion Force in a Temperature Gradient

Hong-Ren Jiang,[1] Hirofumi Wada,[2] Natsuhiko Yoshinaga,[1] and Masaki Sano[1]
[1]*Department of Physics, The University of Tokyo, Hongo 7-3-1, Tokyo 113-0033, Japan*
[2]*Yukawa Insititute for Theoretical Physics, Kyoto University, Kyoto 606-8502, Japan*
(Received 23 February 2009; published 20 May 2009)

The nonequilibrium distribution of colloids in a polymer solution under a temperature gradient is studied experimentally. A slight increase of local temperature by a focused laser drives the colloids towards the hot region, resulting in the trapping of the colloids irrespective of their own thermophoretic properties. An amplification of the trapped colloid density with the polymer concentration is measured, and is quantitatively explained by hydrodynamic theory. The origin of the attraction is a migration of colloids driven by a nonuniform polymer distribution sustained by the polymer's thermophoresis. These results show how to control the thermophoretic properties of colloids.

DOI: 10.1103/PhysRevLett.102.208301 PACS numbers: 82.70.Dd, 66.10.C−, 47.57.J−

Introduction.—Gradients of thermodynamic variables such as temperature, chemical potential, and osmotic pressure cause the migration of molecules and small particles in fluids [1]. For example, in a biological cell, the coupling of two gradients is often used to promote molecular transport against one of the gradients as in chemiosmosis [2]. In physics and chemistry, novel methods to utilize phoretic properties (electro-, thermo-, and diffusiophoresis) are proposed for transporting and screening particles in lab-on-chip [3,4] or designing active materials [5]. In thermophoresis, the speed and direction of migration along a temperature gradient are characterized by the Soret coefficient, which is generally material dependent [6–10]. Diffusiophoresis is a similar phenomenon where colloids move along a gradient of solute concentration [11–13]. The benefits of them have been used for efficient and amplified transport in microfuidics [14–16]. However, strong material dependence of Soret coefficients and difficulty in keeping a stationary solute gradient of diffusiophoresis prevent further development of application of nonequilibrium force by the phoretic effects. There has been marked progress recently in understanding the mechanism of thermophoresis [17–19]; however, it is still challenging to control the magnitude of the force to overcome these problems.

In this Letter, we demonstrate that a suitable coupling of thermophoresis for polymer solute molecules and diffusiophoresis for a target particle (colloid) largely resolve the problems. We report studies on a phoretic motion of colloidal particles in a polymer solution under a temperature gradient. We find that a Soret coefficient of a colloid is sensitive to the polymer (PEG) concentration; as the amount of the polymer increases, the Soret coefficient reverses its sign and its magnitude outweighs by far its intrinsic value. The dependence of the Soret coefficient on the polymer concentration is experimentally determined and is corroborated by our hydrodynamic calculations. This novel effect allows us to transport and trap colloids at any desired position by suitably controlling a temperature distribution and the polymer concentration.

Experiment.—In a thin chamber containing a solution, a steep temperature gradient up to 1 $[\mathrm{K}/\mu\mathrm{m}]$ was created while keeping the local temperature rise quite small ($\Delta T \sim 4$ K) by focusing an infrared laser (Nd:YAG, 1064 nm, power ~4 mW before an objective lens) on a light absorbing metal coated surface of the thin glass chamber (setup I) as shown in Fig. 1(a) [20]. Using this setup, we measured the distributions of polystyrene beads. Figure 1(b) shows fluorescence intensity of 100 nm diameter beads (F8803; Invitrogen) in a water solution. The fluorescence intensity became lower at the hot region around laser focus, indicating polystyrene beads escaped from the hot region due to thermophoresis. The effects of laser trapping and convection are negligible compared with thermophoresis of the beads in this setup. Polystyrene beads and typical bio-

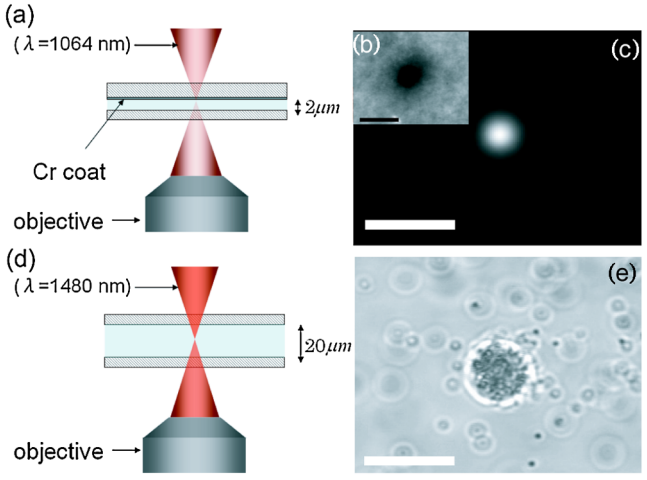

FIG. 1 (color online). (a) Setup I: The laser fed into a thin glass chamber (2 μm) is focused on the top surface coated by a thin Cr layer for light absorption. (b) Distribution of 100 nm fluorescent polystyrene beads in water. (c) Distribution of 100 nm fluorescent polystyrene beads in PEG solution. (d) Setup II: The laser fed into a chamber (20 μm thick) is used for direct aqueous solution heating. (e) Cluster of 500 nm polystyrene beads in PEG solution. Scale bars: 10 μm.

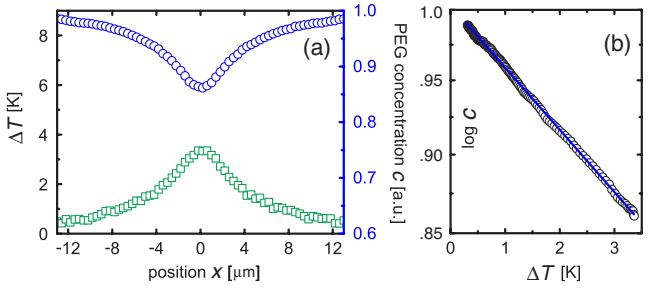

FIG. 2 (color online). (a) Temperature (green or light gray: rectangle, left ordinate) and density of fluorescent PEG (blue or gray: circle, right ordinate) as a function of radius from the center of laser focus. (b) Density of fluorescent PEG vs temperature increment.

molecules such as DNA migrate to colder regions at room temperature [9]. However, when we added a small amount of neutral polymer, polyethylene glycol (PEG6000, MW7500, 3.5 wt %) in 10 mM Tris buffer, beads and DNA molecules [21] migrated and were trapped at the hot region regardless of the sign of thermophoresis [Fig. 1(c)]. The range of attraction reached 5 to 10 μm, corresponding to the size of the temperature distribution [see Fig. 2(a)], exceeding by far about 1 μm in optical tweezers. As we moved the laser or chamber at several micrometers per second, the trapped polystyrene particles moved with the hot region (see the supporting information [22]). This indicated that the sign and the magnitude of thermophoresis were modified in the presence of polymer under a temperature gradient. This effect was also observed in a bulk heating configuration as shown in Fig. 1(d) (setup II). Direct absorption of laser light with longer wavelength (1480 nm, 25 mW, Furukawa) in the water produced a local temperature gradient, which creates a 3D colloidal aggregation within the hot region [Fig. 1(e)].

Polymer distribution.—To elucidate the mechanism of the attraction, in the setup I we measured profiles of temperature and PEG density near the laser focus [23] [Fig. 2(a)]. Since the profiles were axisymmetric, the data shown below are averaged along azimuthal direction. The temperature increment ΔT in the laser heating spot was approximately 1 K with a 1 mW increase in the laser power. We found that the PEG molecules were depleted by about 15% due to PEG thermophoresis when ΔT was about 3 K in the center [Figs. 2(a) and 2(b)]. The depletion of PEG can be described as a steady state distribution by thermophoresis. The flux of PEG molecules obeys the relation

$$\boldsymbol{j}_p = -D^p \nabla c - c D_T^p \nabla T, \tag{1}$$

where c, $\boldsymbol{j}_p$, D^p, D_T^p are the polymer density, flux, diffusion constant, and thermodiffusion constant, respectively. In the steady state ($\boldsymbol{j}_p = 0$), the density satisfies $dc/c = -(D_T^p/D^p)dT = -S_T^p dT$, where the Soret coefficient defined by $S_T^p = D_T^p/D^p$ is measured by $S_T^p = -(1/c) \times (dc/dT) \simeq -\Delta \ln c/\Delta T$. We obtain $S_T^p = 0.046 \pm 0.005$ [K^{-1}] for PEG5000 from the slope in Fig. 2(b), in agreement with Ref. [24].

Trapping ability.—Next we examined how the accumulation of beads is dependent on the concentration of polymer and on ΔT by measuring the density distribution of beads. The fluorescence images of beads were recorded for different PEG6000 concentrations. In Fig. 3, spatial distributions of fluorescent polystyrene beads (100 nm, 0.05%) were displayed. Each image was integrated for 300 frames in 20 sec and was linearly scaled to 256 gray levels. In 0% solution, thermophoresis of beads caused decrease of beads density at the center [Fig. 3(a)]. In 1% solution [Fig. 3(b)], there was still no trapping, but the degree of depletion is diminished compared to the 0% solution. In 2% solution, the trapping phenomenon began to appear and the fluorescence intensity roughly doubled in the hot region [Fig. 3(c)]. In the 3.5% and 5% solutions, the density increased approximately 10- and 100-fold at the center compared with the surrounding concentrations, respectively [Figs. 3(d) and 3(e)].

In Fig. 4, the particle density at each distance from the center is plotted against temperature at the same radius. The result for 0% solution can be described as a steady state distribution due to thermophoresis. The density of beads, n, obeys Eq. (1) with replacement of c by n and S_T^p by S_T^b, where S_T^b is the Soret coefficient of the beads. Neglecting temperature dependence of S_T^b, an exponential distribution is obtained [14]

$$n = n_0 \exp[-S_T^b (T - T_0)]. \tag{2}$$

The slope of the curve in Fig. 4 gives the Soret coefficient as $S_T^b = 0.35 \pm 0.03$ [K^{-1}] in agreement with previous results [9]. Importantly, even in the presence of polymer, the particle density varied exponentially as a function of ΔT (see Fig. 4). Thus a slope of each curve gives an

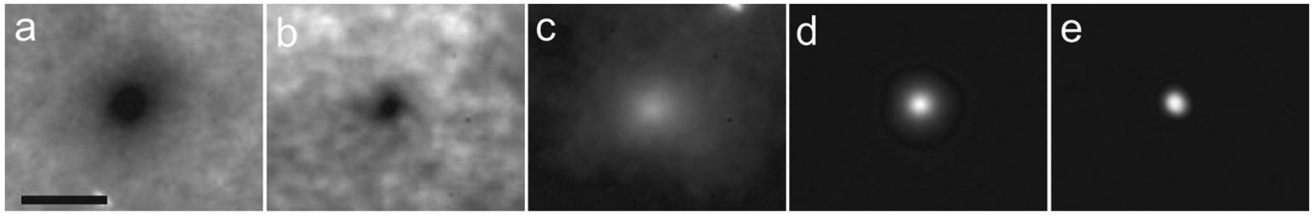

FIG. 3. Fluorescence intensity of 100 nm beads under temperature gradient for different polymer concentrations, (a) 0%, (b) 1%, (c) 2%, (d) 3.5%, and (e) 5% PEG 6000 solutions, respectively. The laser is focused at the center. The scale bar: 10 μm.

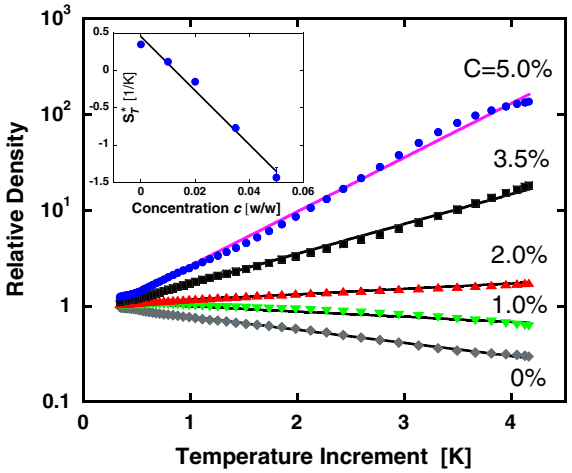

FIG. 4 (color online). The relationship between the temperature increment and the density of the beads divided by its background value, for different PEG concentrations indicated. Filled symbols are the experimental data obtained from Fig. 3. The solid lines are the fits with Eq. (2), from which the effective Soret coefficients S_T^* were obtained. Inset: S_T^* is plotted as a function of the PEG concentration in weight fraction c. The solid line is the fitting with Eq. (6).

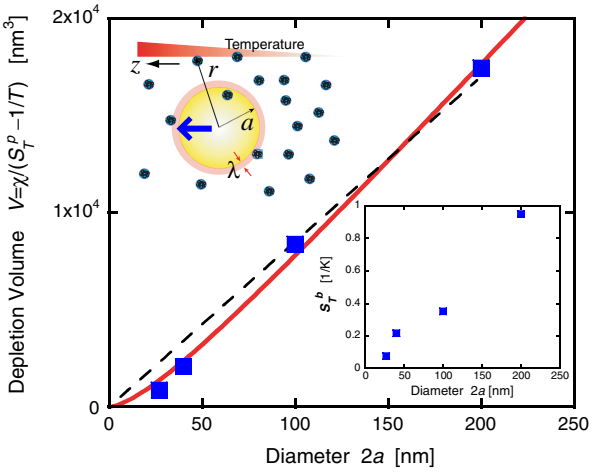

FIG. 5 (color online). Particle diameter dependence of the depletion volume V. Dotted line (solid line): predictions for nonslip (Navier) boundary condition. Insets: (top) schematic illustration of a colloid particle in a polymer solution; (bottom) Soret coefficients of beads for different sizes.

effective Soret coefficient S_T^*. We plot S_T^* as a function of PEG concentration c in the inset of Fig. 4. S_T^* decreased linearly with the increase of polymer concentration c,

$$S_T^* = S_T^b - \chi c \tag{3}$$

with $\chi = 35.4 \pm 2.0\ [\mathrm{K}^{-1}]$ as the best fit for c in weight fraction, or $\chi = 441 \pm 25\ [\mathrm{nm}^3\,\mathrm{K}^{-1}]$ for c in volume density. Hence, the sign and the magnitude of the Soret coefficient were controlled by varying the concentration of polymer.

Theory.—The main results obtained in our experiment are quantitatively explained by the hydrodynamic theories [12,18,19]. We consider a spherical particle of radius a in a polymer solution, see the inset of Fig. 5. In a dilute regime valid to our experiments, PEG distribution around the particle obeys Boltzmann distribution $c = c_0 \exp(-U(r)/k_BT)$, where c_0 is the concentration at infinity, k_B is the Boltzmann constant, and $U(r)$ is a short range potential for PEG molecules. As a PEG is nonionic and inactive, U represents an entropic repulsion from the colloid surface with its interaction distance λ. Note that λ also defines a length scale of the depletion interaction between colloids at equilibrium [25,26]. In a temperature gradient dT/dz applied along z direction, a PEG gradient dc_0/dz is developed according to Eq. (2). As c_0 changes only gradually at a scale of λ, the steady state distribution is given by $c \simeq c_0(z)e^{-U(r)/k_BT}$. Neglecting interactions between polymers, an osmotic force density is given by $\boldsymbol{f} = -c(\boldsymbol{r})\nabla U(\boldsymbol{r})$, which is written in $\boldsymbol{f} = \nabla(k_BT\delta c) + k_BT(S_T^p - \frac{1}{T})\delta c \nabla T$, where $\delta c \equiv c - c_0 = c_0(e^{-U/k_BT} - 1)$, and $\nabla c_0 = -c_0 S_T^p \nabla T$ was used. The velocity field around the colloidal sphere $\boldsymbol{v}$ is obtained by solving the Stokes equation $\eta\nabla^2\boldsymbol{v} = \nabla p - \boldsymbol{f}$, with the incompressibility condition $\nabla \cdot \boldsymbol{v} = 0$, where η is the viscosity of the solution and p is the hydrostatic pressure. The Stokes equation is rewritten as

$$\eta\nabla^2\boldsymbol{v} = \nabla(p - k_BT\delta c) + f_0(r)\boldsymbol{e}_z, \tag{4}$$

where $f_0(r) \equiv k_BT\bar{c}(S_T^p - 1/T)(1 - e^{-U/k_BT})dT/dz$ and $\bar{c} = c_0(z = 0)$. In Eq. (4), the osmotic pressure $k_BT\delta c$ is compensated by a hydrostatic pressure p. (This ensures the absence of osmotic force on the particle proportional to its volume, $\sim k_BTa^3\delta c$.) The nonequilibrium force $f_0\boldsymbol{e}_z$ in Eq. (4), on the other hand, is balanced with the shear viscous force $\eta\nabla^2\boldsymbol{v}$, leading to a fluid flow relative to the colloid surface and a phoretic motion of the colloid at a velocity $\boldsymbol{u}$ relative to the fluid at infinity. Solving Eq. (4) in the colloid-reference frame with the no-slip boundary condition, and summing up the resulting fluid stress over the colloidal surface, we obtain the total force acting on the colloid as $\mathbf{F} = -6\pi\eta a\boldsymbol{u} + 4\pi\boldsymbol{e}_z \int_a^\infty r(r-a)f_0 dr$ [18]. This must be zero because no external force is acting on the colloid. Choosing a specific potential of hard-core type (i.e., $U = \infty$ for $a < r < a + \lambda$ and zero otherwise), we finally arrive at

$$\mathbf{u} = \frac{k_BT}{3\eta}\left(S_T^p - \frac{1}{T}\right)\lambda^2\bar{c}\nabla T. \tag{5}$$

Plugging then Eq. (5) into an expression of the density current of colloids, $\boldsymbol{J} = n\boldsymbol{u} - D\nabla n - nD_T\nabla T$ [19], and rewriting it in a form $\boldsymbol{J} = -D\nabla n - nDS_T^*\nabla T$, we see that an effective Soret coefficient is given by

$$S_T^* = S_T^b - 2\pi\left(S_T^p - \frac{1}{T}\right)a\lambda^2\bar{c}, \tag{6}$$

which confirms the linear dependence on c in Eq. (3), where $\chi = 2\pi(S_T^p - 1/T)a\lambda^2$.

Equation (6) is compared with our experimental data in Fig. 4 inset by employing $S_T^p = 0.056$ for PEG with MW = 7500 estimated from [24]. The best fit gives $\lambda \simeq 5.2$ nm, which is close to the PEG gyration radius ~ 3 nm [27]. We consider the agreement satisfactory, as λ should be of the order of a PEG size. A further consistency check was made by looking at the dependence of S_T^* on the particle radius a. To focus only on this dependence of S_T^*, we define an effective depletion volume at nonequilibrium $V = \chi/(S_T^p - 1/T)$. First, we performed the series of experiments for four different colloid sizes, and extracted V from the data on S_T^*, which are plotted in Fig. 5 as a function of the diameter $2a$. The data show an overall linear dependence, and the agreement with the theoretical prediction for no-slip condition, $V = 2\pi\lambda^2 a$, obtained from Eq. (6), is good. Note that we used $\lambda = 5.2$ nm obtained before, and thus no adjustable parameter is assumed. Nevertheless, it would be important to examine effects of slip of the polymer solution upon the enhancement of the Soret effect, since the perfect slip condition predicts a different scaling, $V \sim \lambda a^2$ [19]. A boundary condition for a general slip case is a so-called Navier condition [28], given by $\sigma_t = \eta v_t/\ell$ at $r = a$, where σ_t and v_t are the tangential components of the fluid stress and velocity. The parameter ℓ defines a slip length on the surface (the no-slip or perfect slip limit is attained for $\ell = 0$ or $\ell = \infty$) [29]. In this Navier case we obtain $V \simeq 2\pi a\lambda[a\lambda + 2\ell(a + 2\lambda)]/(a + 3\ell)$. This formula, with $\lambda = 1.5$ nm and $\ell = 9.7$ nm as the best fit, actually improves the agreement with the data for $a < 50$ nm, where the deviation from the linear dependence is observable (see Fig. 5). In our system, therefore, a fluid slip might be relevant for $a < 50$ nm (with a relatively large slip lengh $\ell \sim 10$ nm).

Summary.—We have developed a micromanipulation technique allowing us to invert and amplify the movement of colloid particles due to thermophoresis of polymers induced by laser focusing. The polymer concentration gradient created by thermophoresis causes migration of a particle with a speed determined by the balance between the driving force and the viscous force. This new method based on nonequilibrium effects does not rely on a specific character of particles and polymers, and thus provides further applications for manipulating a diverse range of colloidal particles as well as biological cells and DNA molecules [21,30]. Our technique is also applicable with other water-soluble molecules [31]. We also note that the effect is stronger for PEG with a larger molecular weight at the same monomer concentration as far as it is lower than the overlap concentration.

This work is supported by a Grant-in-Aid for Scientific Research from MEXT Japan.

[1] S. de Groot and P. Mazur, *Non-Equilibrium Thermodynamics* (Dover Publications, New York, 1984).
[2] P. Mitchell, Nature (London) **191**, 144 (1961); see also P. Nelson *et al.*, *Biological Physics: Energy, Information, Life* (W. H. Freeman, New York, 2007).
[3] M. Z. Bazant and T. M. Squires, Phys. Rev. Lett. **92**, 066101 (2004).
[4] J. Janča, J.-F. Berneron, and R. Boutin, J. Colloid Interface Sci. **260**, 317 (2003).
[5] J. R. Howse *et al.*, Phys. Rev. Lett. **99**, 048102 (2007).
[6] M. Giglio and A. Vendramini, Phys. Rev. Lett. **38**, 26 (1977).
[7] B.-J. de Gans *et al.*, Phys. Rev. Lett. **91**, 245501 (2003).
[8] H. Ning *et al.*, J. Chem. Phys. **125**, 204911 (2006).
[9] S. Duhr and D. Braun, Proc. Natl. Acad. Sci. U.S.A. **103**, 19678 (2006).
[10] M. Braibanti, D. Vigolo, and R. Piazza, Phys. Rev. Lett. **100**, 108303 (2008).
[11] J. P. Ebel, J. L. Anderson, and D. C. Prieve, Langmuir **4**, 396 (1988).
[12] J. Anderson, Annu. Rev. Fluid Mech. **21**, 61 (1989).
[13] J. Nardi, R. Bruinsma, and E. Sackmann, Phys. Rev. Lett. **82**, 5168 (1999).
[14] D. Braun and A. Libchaber, Phys. Rev. Lett. **89**, 188103 (2002).
[15] P. O. Staffeld and J. A. Quinn, J. Colloid Interface Sci. **130**, 69 (1989).
[16] B. Abécassis *et al.*, Nature Mater. **7**, 785 (2008).
[17] F. Brochard and P. G. de Gennes, C.R. Acad. Sci. II **293**, 69 (1989).
[18] R. Piazza and A. Parola, J. Phys. Condens. Matter **20**, 153102 (2008); A. Parola and R. Piazza, Eur. Phys. J. E **15**, 255 (2004).
[19] A. Würger, Phys. Rev. Lett. **98**, 138301 (2007).
[20] H.-R. Jiang and M. Sano, Appl. Phys. Lett. **91**, 154104 (2007).
[21] H.-R. Jiang *et al.* (to be published).
[22] See EPAPS Document No. E-PRLTAO-102-071922 for a supplemental movie. For more information on EPAPS, see http://www.aip.org/pubservs/epaps.html.
[23] The temperature was measured by using a temperature-sensitive fluorescent dye, $2', 7'$ bis(2-carboxyethyl)-5(6) carboxyfluorescein (BCECF) [9,14]. The density of PEG molecules was measured by using fluorescently labeled PEG molecules (rhodamin-PEG, MW5000, Nanos).
[24] J. Chan *et al.*, J. Solution Chem. **32**, 197 (2003).
[25] S. Asakura and F. Oosawa, J. Polym. Sci. **33**, 183 (1958).
[26] J. C. Crocker *et al.*, Phys. Rev. Lett. **82**, 4352 (1999).
[27] S. Kawaguchi *et al.*, Polymer **38**, 2885 (1997).
[28] J. Happel and H. Brenner, *Low Reynolds Number Hydrodynamics* (Noordhoff International Publishers, Leyden, 1965).
[29] A. Ajdari and L. Bocquet, Phys. Rev. Lett. **96**, 186102 (2006).
[30] M. Ichikawa, Y. Matsuzawa, and K. Yoshikawa, J. Phys. Soc. Jpn. **74**, 1958 (2005).
[31] We confirmed that polyvinylpyrrolidone (PVP) and sodium polystyrene sulfonate (NaPSS) also work, yet the effect is strongest for PEG.